

Elevation Change of the Greenland Ice Sheet: Reassessment

Curt H. Davis, Craig A. Kluever, Bruce J. Haines

C.H. Davis, Dept. of Electrical & Computer Engineering, University of Missouri, 5605 Troost Ave, Kansas City, MO 64110 USA.

C.A. Kluever, Dept. of Mechanical & Aerospace Engineering, University of Missouri, 5605 Troost Ave, Kansas City, MO 64110 USA.

B.J. Haines, Jet Propulsion Laboratory, California Institute of Technology, 4800 Oak Grove Drive, Pasadena, CA 91109 USA.

Abstract

Elevation change measurements from satellite altimetry for the southern Greenland ice sheet (south of 72 °N) are re-examined after incorporating technical advancements that significantly improve measurement accuracy. After isostatic adjustment, a spatial average of 32,283 crossover points between the Seasat and Geosat altimeters yields a 1.7 ± 0.5 cm/yr growth rate from 1978 to 1988. This is over ten times smaller than previously reported results. Large spatial variations in elevation change from -15 to +18 cm/yr are observed over the ice sheet for the first time. Interannual variations in elevation change of ± 5 to 10 cm/yr are also observed. Given the large spatial and interannual variations in elevation change, the 1.7 ± 0.5 cm/yr growth rate is too small to determine whether or not the Greenland ice sheet is undergoing a long-term change due to a warmer polar climate.

Introduction

Understanding the current state of the polar ice sheets is critical for determining their contribution to sea-level rise and predicting their future response to climate change. Current sea-level estimates attribute a globally coherent rise of 1.8 ± 0.7 mm/yr due to ongoing glacier and ice-sheet melting (1). It is uncertain, however, what the individual contributions of the

Greenland and Antarctic ice sheets are to sea-level rise at this time. The Greenland ice sheet is of particular interest in climate change studies for two reasons. First, it is significantly warmer than the Antarctic ice sheet, where temperatures remain well below freezing over the vast majority of its surface. Second, the potential for polar amplification of a global warming trend in the northern hemisphere is very probable (2). Thus, the Greenland ice sheet is likely to undergo more dramatic change in response to a global warming trend. Because of these important issues, NASA recently began a focused initiative whose primary goal is the measurement and understanding of the mass balance of the Greenland ice sheet (3). Mass balance refers to the rate at which the volume of the ice sheet is changing.

Time series of ice-sheet surface elevations from satellite radar altimeters can be used to study the mass balance of the ice sheets. Zwally *et al.* (4) estimated that the southern portion of the Greenland ice sheet (south of 72 °N) grew at an average rate of 23 ± 6 cm/yr from 1978-1986 by analyzing elevation data from the Seasat and Geosat satellite altimeters. Zwally (5) suggested an increase in precipitation rates caused by a warmer polar climate as a possible cause of the volume growth. These studies have generated considerable discussion among scientists about the magnitude of the growth measurement and its possible cause (6-11). Technical arguments regarding orbit errors, inter/intra-satellite biases, and retracking algorithms have left considerable uncertainty as to the accuracy of the original results.

It is important to point out that when the Greenland growth results were first published, altimetric studies of ice-sheet change were in their infancy. Substantial progress has been made in recent years on important technical issues through the efforts of many investigators crossing various disciplines. Ice-sheet satellite altimetry has now evolved to a sufficient state of maturity that a new examination of these initial results is now in order. In this paper, we re-examine the

elevation change of the Greenland ice sheet using Seasat and Geosat altimeter data after incorporating important technical advancements.

Methods and Approach

In the original study by Zwally *et al.* (4), the Geosat x Seasat comparison used orbit solutions derived from different gravity models. This was one factor in the incorporation of a 40 ± 40 cm systematic correction (plus uncertainty) in their analysis. Since then, several consistent sets of orbit solutions have been developed for both Seasat and Geosat datasets. This has significantly reduced the radial orbit error and corresponding error estimates for ice elevation change rates.

The Joint Gravity Model-3 (JGM-3) (12) orbit solutions are used in our study and are currently available for Seasat, Geosat-Geodetic Mission (GM), and the Geosat-Exact Repeat Mission (ERM) (13) satellite datasets. The JGM-3 solutions offer an average reduction in radial orbit error (14) anywhere from 20-60 cm (Table 1) when compared to previous solutions. It should also be noted that the new solutions can remove systematic orbit errors present in earlier orbit solutions that could lead to erroneous elevation-change results.

All ice-sheet altimeter data must be post-processed to produce accurate surface elevation measurements. This post-processing is called "retracking" and is required because the leading edge of the ice-sheet return pulse deviates from the on-board tracking gate, causing an error in the telemetered range measurement. Retracking altimetry data is achieved by computing the departure of the waveform's leading edge from the altimeter tracking gate and correcting the satellite range measurement (and surface elevation) accordingly. By comparing the repeatability of surface elevations produced from different ice-sheet retracking algorithms, Davis (8)

demonstrated that the retracking algorithm (15) used by Zwally *et al.* (4), hereafter referred to as the NASA algorithm, introduced significantly larger errors in the elevation data than did three other retracking algorithms. More important, the study showed that the NASA algorithm produced ice-sheet growth rate estimates 30-50% larger than those derived from three competing algorithms, which all produced nearly identical results. Several refinements of the NASA algorithm have been made since the original study (16). However, a recent analysis has shown that the current NASA algorithm (NASA-V4) is still a significant source of random error in the ice-sheet datasets (17).

Table 2 provides a summary of the performance of various ice-sheet retracking algorithms computed using Greenland crossover datasets. The ice datasets use the JGM-3 orbit solutions and crossovers were formed when the time difference between the satellite crossing tracks was less than 30 days. To eliminate data outliers, a 3 SD edit with SD convergent to 2% was used on the crossover residuals (18). The results in Table 2 show that the threshold algorithm offers a reduction in average error of 18-35 cm relative to the other retracking algorithms. The level of improvement is comparable to that obtained by using the latest JGM-3 orbit solutions. The threshold algorithm was developed specifically for measurement and detection of ice-sheet elevation change (17), and elevations produced from this retracking algorithm are used in this study.

Previous ice-sheet elevation studies have relied upon a local or regional approach for analyzing altimeter orbit errors and deriving various orbit error corrections (19). Typically, a reference ocean surface in the vicinity of the ice sheet (e.g. the North Atlantic for Greenland) is created and the orbits of the altimeter satellites over this reference surface are analyzed to derive the orbit error corrections. While suitable for removing orbit error in some applications, this

approach cannot fully exploit the fundamental nature of the orbit error. First, the predominant radial orbit error is a long-wavelength signal concentrated at the circular frequency of the orbital period (1/rev frequency). Second, within each continuous orbit solution arc the phase and amplitude of the 1/rev errors change gradually over large distances, maintaining a very high level of correlation from one revolution to the next (20). Therefore, a global analysis of ocean altimeter data is required to exploit these inherent characteristics.

While a significant amount of effort is required to assemble and analyze a global altimeter database, this type of analysis offers several unique advantages that cannot be achieved using a regional analysis of orbit error. First, a global analysis will unveil correlations and long-period (seasonal to interannual) time-dependent variations in the 1/rev orbit errors. This class of orbit error can manifest itself as a long-term geographically coherent trend in geophysical estimates (21). Second, robust optimal estimation filters can be designed specifically to separate orbit errors at the 1/rev frequency from true geophysical signals in the data. Finally, systematic biases that may be present in inter-satellite comparisons (e.g. Geosat x Seasat) can be characterized separately from the orbit errors. Thus, in this study we adopt a global treatment of the ocean altimeter data to characterize and reduce the predominant long-wavelength orbit errors. This is the first ice-sheet elevation study to incorporate such an analysis of orbit error.

Orbit Error Analysis

The global ocean altimeter datasets used in the orbit error analysis were provided by the NASA Ocean Altimeter Pathfinder program (22). A consistent reference frame (ITRF) and gravity model (JGM-3) were used to calculate the orbits for both the Seasat and Geosat satellites. In addition, a consistent set of atmospheric and geophysical corrections were used

whenever possible. In general terms, our approach was to identify the radial orbit errors by passing time-ordered global sea-surface height residuals through a stochastic filter designed for estimating geophysical and orbital parameters from Global Positioning System (GPS) data (23). The orbit errors were parameterized by sine and cosine functions with periods of one orbital revolution and time-varying amplitudes within each orbit solution (typically 6 d for Seasat and Geosat). The time-varying amplitudes were treated as stochastic processes and determined by the estimation software. The effective removal of orbit error was achieved by tuning various filter parameters, such as the steady-state standard deviation and the decorrelation time for the stochastic process. By properly tuning the filter, an adequate trade-off between removing the 1/rev orbit error and preserving the true underlying geophysical signals was obtained. In addition to estimating the 1/rev orbit errors, the stochastic filter can identify measurement system biases that may be present in inter-satellite comparisons. This feature was utilized to remove instrument biases identified in the global ocean sea-levels between the Seasat and Geosat-ERM data.

To form a reference ocean surface for this study, we performed a collinear orbit error analysis (20) on the Geosat-ERM dataset and subsequently averaged the first two years (43 cycles) of the corrected ERM residuals. Only the first two years of the ERM mission were used for the reference surface since the orbit solutions were degraded by solar activity starting with repeat cycle 44. Next, two global ocean crossover datasets were computed by crossing Geosat-ERM and Seasat data with the reference surface. Orbit corrections based on the crossover data were then derived for each satellite using various filtering strategies to estimate the 1/rev orbit errors. The nominal scheme treated the sinusoidal amplitude coefficients as colored-noise processes with correlation times of 6 days (24). In an alternate scheme for

modeling the 1/rev orbit errors, we used a white-noise process with the amplitude coefficients completely decorrelated from one revolution to the next. As expected, this approach leads to the largest reduction in SD of the ocean crossover data (Table 3). Further analysis of this approach, however, suggested that an unacceptable level of true ocean signal was absorbed into the orbit-error coefficients (25). This was later confirmed in the evaluation of the ice-sheet data, which exhibited higher scatter when the white-noise coefficients were adopted in place of those from the nominal (colored noise) case.

In addition to the 1/rev orbit error coefficients, the filter parameter set for each Seasat orbit solution included a bias parameter to account for a global scale difference between Geosat and Seasat sea-surface heights. Evaluation of the bias estimates showed that Seasat sea levels were on average 29 cm lower than the ERM ocean surface. As global mean sea-level rise during the period between Seasat and Geosat could at most account for 2 cm, we attribute the 29 cm difference primarily to instrument bias between the two satellites.

Ice-Sheet Elevation Change

The Seasat (6 July - 10 Oct 1978) and Geosat-ERM (9 Nov 1986 - 11 Nov 1988) Greenland datasets were provided by the NASA Ice Sheet Altimeter Pathfinder program. Both satellites provided coverage up to a maximum latitude of 72 °N. The ice-sheet surface elevations were produced using the same JGM-3 orbit solutions applied to the ocean altimeter datasets, and thus are referred to the same terrestrial reference frame. Only the first two years (43 cycles) of the ERM data were utilized as solar activity seriously degraded the performance of the satellite beyond this time. Orbit adjustments (26) and the Seasat relative bias estimates (27) from the stochastic filter were applied to the data. Ice-sheet elevation differences were computed by

crossing the ERM and Seasat datasets. A small correction was applied to each elevation difference to correct for slight altitude differences between the two satellites (28).

Results from the ERM x Seasat elevation change study are shown in Table 4. The first two datasets (87 x S, 88 x S) used the same 3-month time period for the ERM and Seasat data to avoid seasonal biases. The last dataset (ERM x S) used the first two years of the ERM data with all the Seasat data to provide a larger number of crossovers (N) and a better spatial distribution. Note that the inclusion of a full two years of ERM data will also tend to average out seasonal variations. The regular dH/dt analysis is simply the average change in elevation (dH) divided by the average time interval (dt) using all the crossovers (29). The spatial dH/dt analysis grids the data into 50 x 50 km cells and computes a spatial average using the mean dH and dt in each cell (30). This is done because the regular dH/dt analysis will be biased towards the northern interior of the ice sheet due to the non-uniform distribution of the satellite tracks (5). Error bounds are reported as ± 1 SD and characterize the uncertainty due to random measurement errors (31). The results for all datasets and both types of dH/dt analysis are consistent, with growth rates from 1-3 cm/yr. These growth rates are nominally ten times smaller than the original results given by Zwally *et al.* (4).

The slightly positive elevation change results represent the average response of the southern Greenland ice sheet. However, these are somewhat misleading as analysis of the spatial distribution of the crossover data indicates that there are large geographic variations in the dH/dt values (Fig. 1). The dH/dt values for the northern interior of the ice sheet are quite small (-2 to +2 cm/yr) and are consistent with estimates showing no significant change in mass balance (32). Thinning of 3-10 cm/yr is indicated for the lower elevations of the eastern and western flanks of the ice sheet between 70-72° N. The thinning along the western flank is supported by

observations showing a retreat of the western margin of the ice sheet around the Jakoshabvn glacier (33). The growth rates west of the ice divide between 65-69 °N vary from 10-15 cm/yr. These agree well with growth rates derived from a comparison of airborne laser altimeter and geociever ground survey data spanning the period from 1980 to 1993/94 (34). In addition, modest thinning is indicated by the few grid cells east of the ice divide between 63-67 °N, which is also consistent with the laser altimeter results (34). However, confidence of thinning in this area east of the ice divide is low due to the poor spatial coverage. The large spatial variation in the growth rates (-15 to +18 cm/yr) contradicts earlier results where large growth rates (>20 cm/yr) were reported for all elevation and latitude bands (5).

The spatially averaged result for the growth of the southern Greenland ice sheet (south of 72 °N) from 1978 to 1987-88 is 2.2 ± 0.5 cm/yr. After correcting for isostatic adjustment (35), the spatially averaged growth rate is 1.7 ± 0.5 cm/yr. The 0.5 cm/yr uncertainty accounts for only the random component of the error. Application of orbit corrections from extreme filtering strategies suggests that the systematic contribution to the rate estimate from the residual orbit errors does not exceed 0.5 cm/yr (36). Uncertainties in the vertical crustal motion, knowledge of the relative instrument bias (37), and biases in the environmental corrections likely contribute at the same level. Considering these sources of systematic error, the small 1.7 cm/yr growth rate estimate may be consistent with a null growth rate. We note that over 95% of the data used in this study occurs at elevations greater than 2000 m. Thus, no conclusion can be made as to the behavior of the lower elevations nearer the ice-sheet margin. We note that natural fluctuations in snow-accumulation rates can also cause decadal changes in surface elevation (11). Our own analysis of interannual variations in ice-sheet surface elevation from the ERM dataset indicates natural fluctuations of ± 5 to 10 cm/yr. Given the large spatial and interannual variations present

in the elevation-change results, we believe the 1.7 ± 0.5 cm/yr growth rate is far too small to assess whether or not the Greenland ice sheet is undergoing a long-term change due to a warmer polar climate as was previously suggested (5). Unambiguous detection of long-term mass balance trends associated with climate change will likely require satellite altimeter time series of ice-sheet surface elevations be extended to two or three decades.

LIST OF TABLES

Table 1. Typical SD of Ocean Crossover Differences for Various Altimeter Orbit Solutions

Gravity Model	Seasat SD (cm)	Geosat - ERM SD (cm)	Avg. Error Increase Relative to JGM-3 (cm)
GEM-T2	60	60	52 / 59
JGM-2	40	25	26 / 22
JGM-3	30	12	-- / --

Table 2. Typical SD of Ice-Sheet Crossover Differences for Various Retracking Algorithms

Algorithm	Geosat - GM SD (cm)	Geosat - ERM SD (cm)	Avg. Error Increase Relative to Threshold (cm)
NASA-V4	41	46	29 / 35
ESA	34	36	18 / 20
Threshold	29	30	-- / --

Table 3. Weighted SD of Global Sea-Height Residuals from Crossover Analysis

Dataset	Uncorrected SD (cm)	Colored-Noise Filter SD (cm)	White-Noise Filter SD (cm)
Seasat x Ref. Surface	27.3	11.7	11.0
ERM x Ref. Surface	10.4	9.1	8.3

Table 4. ERM x Seasat Elevation Change Results

Dataset	Regular dH/dt Analysis				Spatial dH/dt Analysis			
	dH (cm)	dt (yr)	N	dH/dt (cm/yr)	dH (cm)	dt (yr)	N	dH/dt (cm/yr)
87 x S	16 ± 7	9	4,277	1.8 ± 0.8	23 ± 7	9	3,539	2.5 ± 0.8
88 x S	23 ± 12	10	2,789	2.3 ± 1.2	3 ± 12	10	1,908	0.3 ± 1.2
ERM x S	9 ± 3	9.25	32,867	1.0 ± 0.3	20 ± 5	9.25	32,283	2.2 ± 0.5

LIST OF FIGURES

Figure 1. Spatial distribution of elevation change from 1978-1988 showing large variations in dH/dt values. The approximate location of the ice divide is indicated by the series of stars. A spatial average yields a mean growth rate of 2.2 ± 0.5 cm/yr.

REFERENCES AND NOTES

1. W.R. Peltier and A.M. Tushingham (1989), "Global sea level rise and the greenhouse effect: might they be connected?" *Science*, Vol. 244, pp. 806-810.
2. E. Barron (1995), "Forum on global change modeling," *USGCRP Report 95-02*, Washington, DC.
3. W. Abdalati (1996), *Program for Arctic Regional Climate Assessment (PARCA) - Greenland Science and Planning Meeting*, CIRES, University of Colorado, Boulder, CO, 17-18 Sept 1996.
4. H.J. Zwally, A.C. Brenner, J.A. Major, R.A. Bindschadler, and J.G. Marsh (1989), "Growth of Greenland ice sheet: measurement," *Science*, Vol. 246, pp. 1587-1589.
5. H.J. Zwally (1989), "Growth of Greenland ice sheet: interpretation," *Science*, Vol. 246, pp. 1589-1591.
6. B.C. Douglas, R.E. Cheney, L. Miller, R.W. Agreen (1990), "Greenland ice sheet: is it growing or shrinking?," *Science*, Vol. 248, pg. 288.
7. H.J. Zwally, A.C. Brenner, J.A. Major, R.A. Bindschadler, and J.G. Marsh (1990), "Response - Greenland ice sheet: is it growing or shrinking?," *Science*, Vol. 248, pp. 288-289.
8. C.H. Davis (1995), "Growth of the Greenland ice sheet: a performance assessment of altimeter retracking algorithms," *IEEE Transactions on Geoscience & Remote Sensing*, Vol. 33, No. 5, pp. 1108-1116.
9. S.H. Schneider (1992), "Will sea levels rise or fall?" *Nature*, Vol. 356, No. 5, pp. 11-12.
10. R.J. Braithwaite (1993), "Is the Greenland ice sheet getting thicker?" *Climatic Change*, Vol. 23, pp. 379-381.

11. C.J. Van der Veen (1993), "Interpretation of short-term ice-sheet elevation changes inferred from satellite altimetry," *Climatic Change*, Vol. 23, pp. 383-405.
12. B.D. Tapley *et al.* (1996), "The joint gravity model 3," *J. Geophys. Res.*, Vol. 101, pp. 28209-28409.
13. R.G. Williamson and R.S. Nerem (1994), "Improved orbit computation for the Geosat mission: benefits for oceanographic and geodynamic studies," *EOS Trans. Suppl.*, p. 155.
14. The average reduction in error is defined as the square-root of the difference between the squares of the larger SD (e.g. GEM-T2) and the smallest SD (JGM-3). This quadrature difference is sometimes referred to as the root-difference-square (RDS).
15. T.V. Martin, H.J. Zwally, A.C. Brenner, and R.A. Bindshadler (1983), "Analysis and retracking of continental ice sheet radar altimeter waveforms," *J. Geophys. Res.*, Vol. 88, pp. 1608-1616.
16. For example, H.J. Zwally, A.C. Brenner, J. DiMarzio, and T. Seiss, "Ice sheet topography from retracked ERS-1 altimetry," *Proceedings of Second ERS-1 Symposium*, ESA SP-361, pp. 159-164, 1994. For a complete description of the evolution of the NASA retracking algorithm see: GSFC Ice-sheet Pathfinder Homepage, http://crevasse.stx.com/ia_home, 1996.
17. C.H. Davis (1997), "A robust threshold retracking algorithm for measuring ice-sheet surface elevation change from satellite radar altimeters," *IEEE Transactions on Geoscience & Remote Sensing*, Vol. 35, No. 4, pp. 974-979.
18. A small number of data outliers are present in ice-sheet altimeter datasets due to irregular ice-sheet topography (see Note 5 in (4)).
19. For example, H.J. Zwally *et al.* (1990), "Satellite radar altimetry over ice: processing and corrections of Seasat data over Greenland," *NASA Ref. Pub. 1233*, Vol. 1, NASA Scientific and

- Technical Information Division; C.S. Lingle *et al.* (1994), "Recent elevation increase on Lambert Glacier, Antarctica, from orbit crossover analysis of satellite-radar altimetry," *Annals of Glaciology*, Vol. 20, pp. 26-32.
20. For example, D.B. Chelton and M.G. Schlax (1993), "Spectral characteristics of time dependent orbit errors in altimetry height measurements," *J. Geophys. Res.*, Vol. 98, pp. 12579-12600.
21. An ice-sheet growth rate of 28 cm/yr was reported by Zwally *et al.* (4) based on an analysis of Geosat x Geosat crossover data. Douglas *et al.* (6) report a secular increase of 50 cm/yr for the North Atlantic sea level using the same dataset (see also Fig. 7 in R.E. Cheney *et al.* (1991), Geosat Altimeter Crossover Difference Handbook, NOAA Manual NOS NGS 6, Rockville, MD). Both the ice-sheet and sea-level trends are unrealistic and are likely due to time-dependent orbit error variations.
22. Ocean Pathfinder Homepage, <http://neptune.gsfc.nasa.gov/ocean.html>
23. S.M. Lichten (1990), "Estimation and filtering for high-precision GPS positioning applications," *Manuscripta Geodaetica*, Vol. 15, pp. 159-176.
24. This strategy is designed to capture most of the time-varying 1/rev radial orbit error without significant loss of geophysical signal. The selection of a long time constant also prevents the filter from accommodating the stationary gravity-induced orbit error which is manifest in crossover residuals (see for example, B.D. Tapley and G.W. Rosborough (1985), "Geographically correlated orbit error and its effect on satellite altimetry missions," *J. Geophys. Res.*, Vol. 90, pp. 11817-11831). We prefer these errors remain in both the reference surface and sea-height residuals. The orbit characteristics of Seasat and Geosat are nearly identical and thus this class of orbit error will largely cancel in comparisons between two missions as long as

the region in question is represented by nearly equal numbers of ascending and descending tracks with respect to the reference.

25. Global ocean images of sea height (referenced to the mean surface) were created for all ERM cycles. Sequential time-series of these images were analyzed to determine whether or not the orbit corrections removed known geophysical signals (e.g. the 1986-87 El Nino).

26. Orbit corrections over the ice sheet are obtained by extrapolating the sinusoidal orbit-error functions. The SD of the 1/rev orbit adjustments applied to the ERM x Seasat ice-sheet crossover data were 21 cm and 4.7 cm for the Seasat and Geosat data, respectively. After applying the orbit corrections, the SD of the ice-sheet crossovers was reduced from 44.5 to 37.0 cm, which implies an average reduction in radial orbit error of 24.7 cm. This is consistent with the 24.7 cm reduction in orbit error for the global Seasat ocean dataset, which is the primary source of orbit error in the ERM x Seasat ice-sheet data.

27. There were seventeen separate Seasat orbit solutions used in our study. The mean and SD of all systematic biases applied to the Seasat data was 29 ± 2.6 cm.

28. The nominal orbit altitude for both Seasat and Geosat was 800 km, but small differences between the orbital heights (± 5 km) did occur for a given point on the ice-sheet surface. Over a flat surface, the change in elevation computed from two different satellites (A and B) is $dH = H_B - H_A$, where H_B and H_A are the surface elevations located at the same point (nadir) on the ice-sheet surface. Over a sloping ice-sheet surface, the location of the closest point to the surface will be different for satellites with different orbital heights. In this case, $dH = H_B - \Delta - H_A$, where $\Delta = (OH_B - OH_A) \sin^2\alpha$, OH are the orbital heights, and α is the regional ice-sheet slope. The regional slope was determined using a 10 km x 10 km slope grid computed from a

digital elevation model of Greenland produced by S. Ekholm at Kort-og Matrikelstyrelsen, Denmark. The mean and SD of all corrections applied to 35,600 ERM x Seasat dH values was -2.8 ± 9.0 cm.

29. The ascending-descending (A-D) orbit bias is accounted for by using the method described by Zwally *et al.* (4). In addition, crossover differences greater than 3 SD of the primary Gaussian distribution were discarded to eliminate data outliers (see Note 5 in (4)).

30. For a cell to be used a minimum number of ten crossovers had to be present, with at least five from Geosat-Seasat (A-D) and five from Seasat-Geosat (A-D).

31. The distribution of the mean dH value is approximately Gaussian for both the regular and spatial dH/dt analysis.

32. J.F. Bolzan, "A glaciological determination of the mass balance in central Greenland," *EOS Trans. Suppl.*, Vol. 73, No. 43, p. 203.

33. H. Sohn, K. Jezek, and C. Van der Veen (1997), "Jakoshavn glacier, West Greenland: 30 years of spaceborne observation," *Science*, submitted.

34. W. Krabill, R. Thomas, K. Jezek, K. Kuivinen, and S. Manizade (1995), "Greenland ice sheet thickness changes measured by laser altimetry," *Geophys. Res. Lett.*, Vol 22, No. 17, pp. 2341-2344.

35. A correction for the vertical velocity of the ice base due to crustal deformation was subtracted from the dH/dt value of each 50 x 50 km cell and the spatial average was recalculated (see http://cfageod4.harvard.edu/calc_def.html for details of the vertical velocity calculations). The mean of the correction was 0.5 cm/yr.

36. In the two extreme filtering strategies, the 1/rev orbit error amplitude coefficients were modeled as 1) constant parameters throughout the entire orbit solution (typically 6 d) and 2)

white-noise processes with no correlation from one orbital revolution to the next. The nominal estimate of the overall ice-sheet growth rate was altered by +0.4 and -0.3 cm/yr for cases 1 and 2, respectively.

37. The relative instrument bias is estimated from the global ocean data and as such is not perfectly separable from the sea-state bias resulting from the non-coincidence of electromagnetic and geometric sea level as well as tracker and skewness biases. We estimated a global sea-state bias for Seasat as a percentage of the significant wave height. Comparison of different sea-state models for the Topex altimeter suggests that residual mismodeling of sea-state effects may impact the instrument bias at the 2-3 cm level (see for example Table 6 of E.J. Christensen *et al.* (1994), "Calibration of Topex/Poseidon at platform Harvest," *J. Geophys. Res.*, Vol. 99, pp. 24465-24485). A 3-cm error in the relative bias translates to 0.3 cm/yr in terms of the overall ice-sheet growth rate.

38. We are grateful to R. Thomas for his continued support of this work. We thank the NASA Pathfinder Program for the ocean and ice sheet altimeter datasets; in particular we acknowledge the help of H.J. Zwally, C. Koblinsky, A. Brenner, J. DiMarzio, and B. Beckley for their assistance in obtaining these data. This research was supported by funds from NASA's Office of Mission to Planet Earth under grants NAGW-5010 and NAGW-5243. A portion of the work in the paper was conducted by the Jet Propulsion Laboratory, California Institute of Technology under contract with NASA on RTOP #622-83-1740.

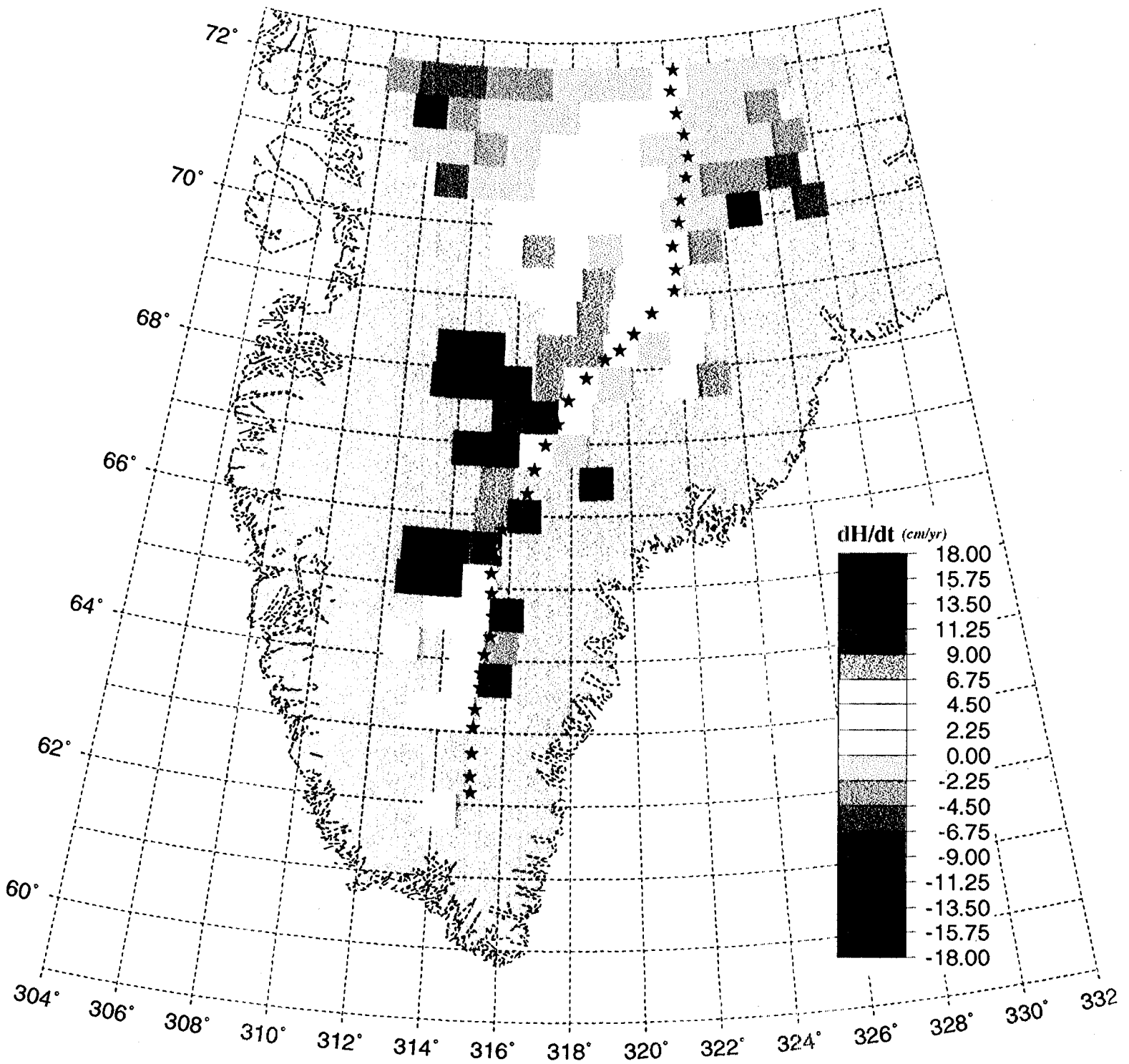


Figure 1. Spatial distribution of elevation change from 1978-1988 showing large variations in dH/dt values. The approximate location of the ice divide is indicated by the series of stars. A spatial average yields a mean growth rate of 2.2 ± 0.5 cm/yr.